

ELECTRO-OPTICAL PROPAGATION: POINT AND PATH-AVERAGED TRANSMISSION MEASUREMENTS

Alexander M.J. van Eijk^(1,2,3), Peter Grossmann⁽²⁾, Erik Sucher⁽²⁾, Faith J. February⁽⁴⁾, and Karin Stein⁽²⁾

⁽¹⁾*Fraunhofer Institute for Optronics, System Technologies and Image Exploitation (ISOB),
Gutleuthausstrasse 1, 76275 Ettlingen, Germany;*

⁽²⁾*TNO, P.O.Box 96864, 2509 JG The Hague, The Netherlands, Email: lex.vaneijk@tno.nl;*

⁽³⁾*LHEEA (UMR CNRS 6598), Ecole Centrale de Nantes, 1 Rue de la Noë, 44300 Nantes, France;*

⁽⁴⁾*Institute for Maritime Technology (IMT), Simons Town, South Africa;*

KEYWORDS: experiment, scintillometer, transmissometer, optical particle counter, transmission, MODTRAN

ABSTRACT:

The concentration and composition in the Earth's atmosphere varies substantially in space and time. Our efforts focus on assessing the impact of this inhomogeneity on the transmission over optical propagation links. In particular, we focus on the error that is made when assuming default aerosol properties, and we investigate the representativeness of point measurements for characterizing an optical link of multiple kilometres.

1. INTRODUCTION

Electro-optical sensors are presently used for a wide range of applications in the marine environment, e.g., for surveillance, ranging, and classification. The performance of state-of-the-art sensors is generally not determined by system design and technological limitations, but rather by the intervening atmosphere. The molecules and aerosols present in the atmosphere scatter and absorb radiation, thereby reducing the amount of radiance from an object that reaches the sensor. While target radiance is scattered out of the field-of-view (FOV) of the sensor, the aerosols may also scatter a fraction of the solar radiation into the sensor (stray light or path radiance), resulting in an additional non-target radiation load onto the sensor and a reduction in target-background contrast [1]. Transmission losses and contrast reduction result in a decreased image quality and reduced detection, recognition and identification (DRI) ranges.

The atmospheric molecules and aerosols also affect the electro-optical signature of an object. The absorption and scattering process results in a radiative load onto the object that differs from the nominal solar radiation reaching the top of the Earth's atmosphere. In general, this will reduce lead to less heating of the object, thereby reducing the (longwave) infrared signature of the target. Likewise, there is generally less solar radiation reflected off the target, thereby reducing the visual signature of the target.

For engineering purposes (e.g., sensor performance), these effects are generally assessed with the MODTRAN code, initially developed by the US Air Force [2]. The code estimates the composition and concentration of molecules and aerosols along the optical path, the amount of incident (source) radiation, and then generates parameters such as the radiative load onto a target, transmission along the optical path, and path radiance. This task is relatively easy for the molecular contribution, since the molecular composition and concentration of the atmosphere are relatively constant (apart from water vapor) and the scattering and absorption characteristics of the various molecular species are well-known. However, the aerosol composition and concentration are much more variable. Since the experimental assessment of these quantities is not straightforward and tedious, substantial efforts have been reported to develop models that provide the aerosol component as function of geophysical parameters (location, meteorology) [see, e.g., 3-6].

MODTRAN includes a number of default atmospheres and predefined aerosol models that serve users who do not have a complete atmospheric characterization available for the specification of MODTRAN's input parameters. This obviously introduces an uncertainty in the results, and over the last few years we have endeavored to quantify the error thus made. Initially [7], we reported on a theoretical exercise of running MODTRAN in various configurations. Subsequently [8], we compared the MODTRAN results to experimental transmission data acquired at a test range in Meppen, Northern Germany. These comparisons forced us to consider the homogeneity of the range, since the comparison data originated both from point measurements and path-averaged measurements. The concept of homogeneity was further explored in a more challenging environment, i.e., an over-water optical range near a mountainous coast in SimonsTown, South Africa [9].

The present paper continues our efforts to quantify aerosol inhomogeneity and the implications thereof on the use of engineering tools such as MODTRAN or parametric aerosol models. Section 2 briefly

revisits the MODTRAN tests and the comparisons in Meppen, whereas section 3 discusses the FESTER experiments in SimonsTown [10]. Here, we had the rare opportunity of collecting data simultaneously on two separate optical links, with the starting point in common and different end points. One link ran along the coast, the other one perpendicular to the coast, thereby spanning a box of roughly 8 x 2 km. Point observations of the aerosol concentration were made at the common starting point of the two links. Section 4 presents the conclusions of this study.

2. THE MEPPEN TRIAL

2.1 Experimental details

The MEPPEN experiment took place from 15 July – 31 August 2014 at the test range of the Bundeswehr Technical Center for Weapons and Ammunition, WTD 91 in Meppen, North-Western Germany (7°50' E, 52°23'N). As demonstrated by Fig.1, this is a rural site with mostly agricultural land-use. The site includes a well-instrumented meteorological mast [11], from which the standard meteorological data (temperature, humidity, wind, etc) were obtained. An Eltro visibility meter (nr 076-02-77) was also installed here. All data were available as 5-minute averages.

Point aerosol measurements were made by two optical particles counters (OPC) positioned next to the meteorological mast. The OPCs were manufactured by Particle Measurement Systems (PMS), a CSASP-200 and a CSASP-100HV. The two probes provide a diameter range of 0.21 to 45 μm in 91 channels. The raw data from the probes was accumulated over 15 minutes to create a single size distribution considered representative for this time interval. Mie theory was used to convert the size distributions in extinction, from which the transmission over the optical path of 1530 m was obtained with Lambert-Beer's law (see [8] for details).

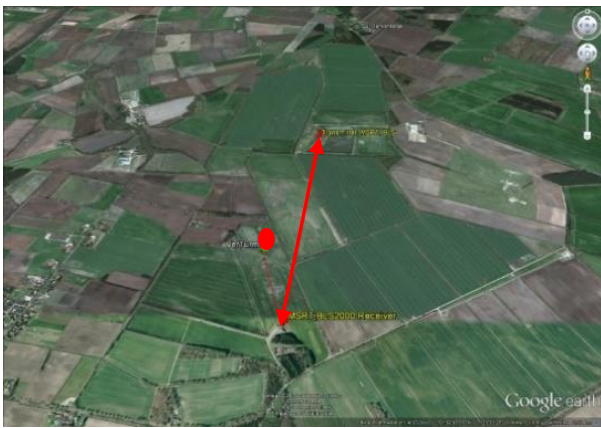


Figure 1: Aerial view of the trial area near Meppen, Germany. The longer red line denotes the optical path of the MSRT and the BLS2000.

A boundary layer scintillometer (Scintec AG / Germany BLS2000) was operated over an optical path of 1530 m length as shown by the longer red line in Fig.1. The BLS systems estimates the integrated turbulence between transmitter and receiver from the intensity fluctuations (scintillation) of a light signal (with a wavelength of 0.88 μm), which are averaged over 1 minute to a direct estimate of the refractive index structure-function parameter C_n^2 . However, the raw data files of the BLS2000 also contain the (corrected) light intensity in the X and Y-directions, reported as average values over 30 seconds. We have shown [8] that this average intensity is a measure for the transmission; normalization was subsequently achieved by searching the maximum intensity over the whole measurement timeframe and setting this maximum equal to the transmission evaluated with MODTRAN (using an user-defined atmosphere, rural aerosols and visibility tuning), for this particular timestamp.

Transmission measurements over the 1.53 km path were also made using the Multi-Spectral Radiometer Transmissometer (MSRT) developed and built by TNO [12]. This instrument provides the transmission in 7 wavelengths bands, one of which corresponds to 0.78 – 1.04 μm . Transmission values were calculated as 1 minute averages of the raw data in volts. Normalization was achieved in a similar manner as for the BLS2000.

2.2 MODTRAN runs

As mentioned before, MODTRAN offers the possibility to use predefined atmospheres, which set the pressure, relative humidity and temperature for the user. Since these parameters had been measured at the meteorological tower, we were able to define user-defined atmospheres for MODTRAN (on a 5-min timestep). The top panel of Fig.2 shows the results of this exercise. The data displayed in Fig.2 spans approximately 4 days, but can be considered representative for the whole experiment – zooming in allows us to show the variations in transmission more clearly. In the first run, we have excluded the aerosols and only calculated the molecular contribution to the transmission at 0.88 μm (the BLS2000 wavelength). The light-blue line at the very top of the panel shows that the transmission over a path of 1530 m exhibits marginal fluctuations. Over the whole timeframe the transmission fluctuated between 0.97 and 1.00, even though the relative humidity varied between 20 and 100%. This shows that water vapor does hardly affect the transmission at 0.88 μm .

A second series of MODTRAN runs was made with the user-defined atmosphere (see above) and the default rural aerosol model provided by MODTRAN, which seemed the most appropriate for the site. MODTRAN provides two predefined visibilities (5 and 23 km), and the 5 km value was selected for

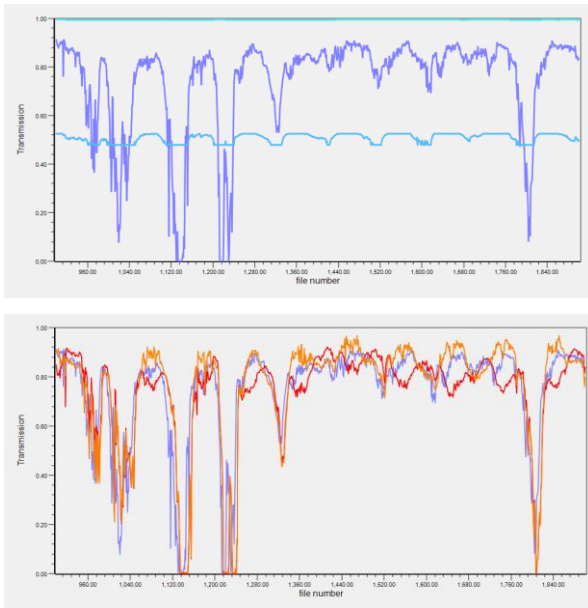


Figure 2: Results for Meppen, Germany. Top panel: MODTRAN runs. Bottom panel: comparison between MODTRAN (blue), BLS2000 (red) and MSRT (brown).

this set of runs. The results are shown by the lightblue line in the middle of the top panel of Fig.2. There are now some fluctuations in the transmission, but more importantly, it can be concluded that the presence of aerosols dramatically reduces the transmission as compared to the molecules-only calculations. This is discussed in more detail elsewhere [7], where it is also shown that selecting another aerosol model (e.g., maritime instead of rural) may lead to substantial changes in the transmission.

Finally, we have run MODTRAN with user-defined atmosphere, the rural aerosol model and the visibility as measured at the meteorological tower. This resulted in the dark-blue lines shown in the two panels of Fig.2. It is evident that the temporal variations in visibility have a strong impact on the transmission at $0.88 \mu\text{m}$. As discussed elsewhere [7], MODTRAN uses the visibility to gauge the aerosol concentration. For the rural aerosol model, visibility is the only meteorological gauge. Other aerosol models (NAM, desert) additionally use wind speed to tune the aerosol concentration, but visibility remains the more important parameter (at least for shorter wavelengths).

2.3 Comparisons

The bottom panel of Figure 2 shows a comparison between the MODTRAN runs (user-defined atmosphere, rural aerosols, visibility tuning), the transmissometer (MSRT) and the carrier signal of the BLS2000. It is evident that MODTRAN captures very well the variations in the measured transmission. A quick glance on the left panel of Fig.2 reveals that MODTRAN only does so when the

(proper) aerosol model is invoked and visibility tuning is applied.

It is noted that MODTRAN is driven with meteorological parameters (pressure, wind, humidity, visibility) that have been acquired at a single point, at or near the meteorological mast (Fig.1), which was located some 100 m from the actual optical path. Since the MSRT and BLS-data represent average conditions over the 1530 m optical path, the good correlation between the three curves in Fig.2 signals relative homogeneous aerosol conditions in the area. In other words, no strong gradients in aerosol concentrations seem to be present over the optical path or in its direct surroundings. This may not be surprising for a flat, rural area in Northern Germany, but may be different in other locations. This is further explored in the next section.

3. THE FESTER TRIAL

3.1 Experimental details

The FESTER campaign took place from April 2015 through February 2016 near Cape Town, South Africa (Fig. 3). The centre location of the trial was the Institute for Maritime Technology (IMT) in Simon's Town, and the area of interest spanned the Northern and North-western parts of False Bay. Two optical links were established from the IMT: one over 1.8 km to the Roman Rock lighthouse (RR), and one over 8.7 km to a sea-facing apartment in St-James (SJ). The longer path was instrumented by the BLS2000 and MSRT (see section 2.1). The shorter path was characterized by three BLS900 systems, with average heights over the water of 7, 15 and 21 meters. We assume that the carrier signals of the BLS-systems again serve as an indicator for the transmission (see section 2.1). Point measurements of the aerosol concentration were made at the IMT using the OPCs discussed in section 2.1. Mie theory was gain used to estimate transmissions over the two optical paths. Meteorological conditions were measured at Roman Rock, where also a Sonic anemometer was installed. The FESTER campaign included more experiments than discussed here; an overview is given elsewhere [10].

3.2 Inhomogeneity

As mentioned before, we expected the FESTER trial to be more inhomogeneous than Meppen. Our assumption was motivated by the typical orography of False Bay, with relatively high (up to 500 m) mountains on either side that create a flow canal for winds that generally come from the South-East or the North (middle panel of Fig.3). One might expect shadowing effects of these nearby mountains in SimonsTown and along the longer optical path to the North. Furthermore, a previous experiment [13] had suggested that the strong spatial variations of the sea surface temperature over the Bay impact on



Figure 3: FESTER trial area. Top panel: global area, the city of Simon's Town is indicated by the marker. Middle panel: Orography of the trial area. Bottom panel: zoom of trial area, IMT = Institute of Maritime Technology, RR = Roman Rock, SJ = St. James. Arrows indicate propagation links.

the local micrometeorological climate and thereby on the near-surface optical paths.

Recently [9], we analysed the MSRT and BLS2000 transmission data (nominally $0.88 \mu\text{m}$) acquired during FESTER and concluded that these two instruments, both deployed over the longer optical path IMT – SJ, agreed generally well, just as they did during the Meppen experiment. An initial comparison of transmission data over the shorter and longer paths with the point aerosol measurements at IMT revealed that the time series globally exhibit the same trends, but that differences exist at specific times. These differences could be

indicative for inhomogeneous conditions over False Bay.

Fig.4 extends our analysis of transmission data. We show here a representative timeframe of approximately three days, where the red and green lines denote the carrier signals of the BLS900 (over the short path IMT – RR) and the BLS2000 (over the long path IMT – SJ), respectively. The signals have been converted into transmission using a procedure similar to the one described above. Due to uncertainties in the aerosol loading over the path, the obtained transmissions should not be taken as absolute values. The main interest of Fig.4 is therefore the comparison of temporal trends.

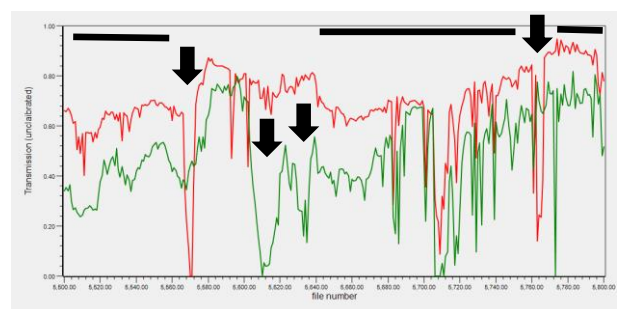


Figure 4: Comparison of carrier signals of BLS900 (operated over the short path) and BLS2000 (operated over the long path) during three representative days of FESTER.

With this in mind, Fig.4 reveals that the two BLS instruments show quite similar behaviour for the better part of the three selected days. The major timeframes of similarity are indicated by the thick black lines at the top of the graph. This behaviour suggests that quite homogeneous conditions existed over the two optical paths. Inspection of the full FESTER dataset led us to believe that this is a general feature for the whole timeframe that the two scintillometers were operated together (roughly 6 months).

On the other hand, the black arrows in Fig.4 point to episodes where a clear distinction exists between the two instruments. As an example, the two middle arrows point to timeframes where the transmission over the long path (green) dropped significantly, whereas the transmission over the short path (red) remained almost unchanged. These episodes last several hours, which rules out the possibility of a single erroneous data point in one of the sensors. Shorter-lived events, e.g. as indicated by the left-most arrow, lasted less than an hour. In this case, the service records should be consulted to exclude the possibility of temporary drops in signal strength due to window cleaning, etc. Again, it should be mentioned that the behaviour shown in Fig.4, i.e., quite good agreement with relative short episodes

of disagreement, seems to a general feature of the whole dataset.

The top panel of Fig.5 shows the same BLS-data as in Figure 4 (red and green curves), but now the data from the PMS aerosol probes has been added (blue curve). These data represent the point measurements at IMT, the common starting point of both optical paths. The transmission values have been calculated for a (hypothetical) optical path of 1 km, by the procedure explained in section 3.1, and only serve for a comparison of temporal trends.

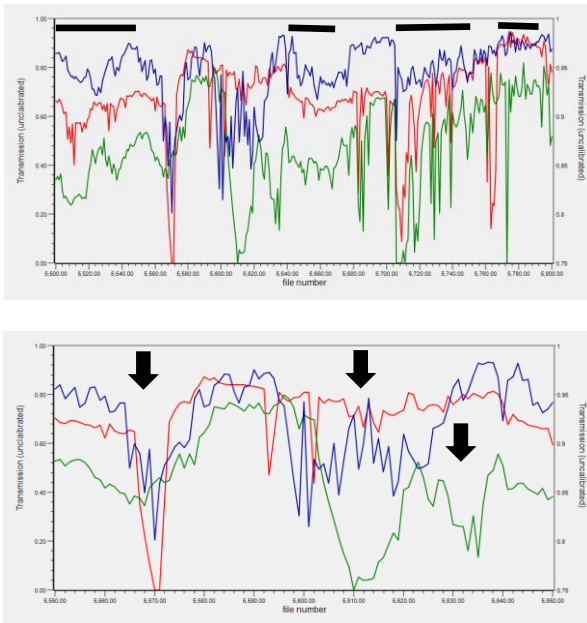


Figure 5: Comparison of PMS transmission data (blue curve), and the carrier signals of BLS900 (red curve, operated over the short path) and BLS2000 (green curve, operated over the long path) during three representative days of FESTER.

The thick black bars in the top panel of Fig.5 identify again timeframes where a quite similar temporal behaviour of the PMS and the two BLS-instruments is observed. While the addition of the PMS slightly reduces the timeframes of similar behaviour (e.g., by breaking up the long middle black line in Fig.4), the conclusion that the three instruments compare surprisingly well over the whole experiments still holds. This preliminary conclusion differs from an analysis of C_n^2 -values over the optical paths [15], where discrepancies between the BLS900 and BLS2000 lasting for several days have been observed.

The bottom panel of Fig.5 shows a zoom of the left panel, covering approximately 25 hours. The zoom focuses on two events where there are discrepancies between the behaviour of the three instruments. The first event, indicated by the arrow on the left, shows a pronounced transmission dip for the PMS(blue) at IMT and the BLS900 (red) over

the shorter path to Roman Rock (RR), which is not (strongly) picked up by the BLS2000 (green) over the longer path to St-James (SJ). Possibly, this signals a fog event (drifting fog banks) close to the IMT building along the line towards the Rock. The second event is flagged by the two arrows on the right of Fig.5. In this case, the BLS900 (red) shows marginal variations in the transmission during the whole event. The BLS2000 (green) shows two pronounced dips in transmission, and it seems that only the first of these dips is picked up by the PMS at IMT.

Obviously, we should look at the meteorological scenario to find explanations for timeframes that our three measurements followed similar or different trends. Since the analysis of the FESTER transmission data is still in its early stages, an extensive meteorological analysis has not yet been completed. So far, we did a quick scan on wind speed and wind direction, but no strong general relations emerged between these parameters and the occurrence of specific events (e.g., BLS900 drops, but BLS2000 does not). It seems that each case must be inspected separately and in detail, before a general pattern (if any) can be established.

4. CONCLUDING REMARKS

The above results may provide some hints about the horizontal aerosol homogeneity in the atmosphere. Both the Meppen and the FESTER trials allow a comparison between path-averaged data and point measurements (at one of the starting point or nearby). The FESTER trial is special because two optical links were established, in nearly perpendicular direction, with the point measurements at the common starting point. Also, while the Meppen trial took place in a fairly homogeneous rural area (Fig.1), the optical paths during FESTER (Fig.3), along and perpendicular to a mountainous coast, over waters with varying sea surface temperature, carried all elements for inhomogeneous conditions.

Nevertheless, the point and path-averaged measurements showed remarkably similar temporal behaviour for most of the time, both in Meppen and during FESTER. Significant differences were almost exclusively observed for the FESTER dataset, and if so, especially between BLS900 operated over the shorter path to the East (Roman Rock lighthouse) and the BLS2000 operated over the longer path to the North (apartment in St James). This corroborates with our understanding of the probability of encountering inhomogeneous conditions. Interestingly, more often than not, the point measurements by the PMS aerosol probes at IMT correspond with at least one of the BLS-curves. This suggest that the cause of the different behaviour of the two BLS-instruments should be sought over the paths, and not at the IMT-building.

Fig.3 shows that the two optical paths established during FESTER can be considered as the two sides of a semi-rectangle of roughly (1.8 * 8.7 =) 15 km². Speculatively, the strong similarity in temporal behaviour of the two BLS-instruments then suggest that the scale of aerosol inhomogeneity is generally greater than, say, 5 to maybe 10 km. It is obvious that this rough order of estimate may only apply to the SimonsTown area, or even to the specific conditions encountered during FESTER. It should also be mentioned that this scale of inhomogeneity applies to an engineering parameter, i.e., transmission over a path of several kilometres. There may very well be inhomogeneities in aerosol concentration and composition on scales smaller than the aforementioned 5 km, but apparently these variations do not significantly affect the overall transmission.

The speculation presented inspires us to continue our experimental efforts to establish multiple links in the same general area, to increase our dataset on inhomogeneity in aerosol transmission. In parallel with our experimental program, we also maintain a modelling effort. Interestingly, the inhomogeneity scale mentioned above falls within the current grid resolution of numerical aerosol transport models, such as WRF-Chem or LOTOS-EUROS. Therefore, we intend to complement our FESTER analysis with modelling efforts of the larger mesoscale flow around False Bay.

5. ACKNOWLEDGEMENTS

The work of Fraunhofer-IOSB was supported and funded by the Bundeswehr Technical Center for Weapons and Ammunition, WTD 91 in Meppen. The authors acknowledge the their helpful colleagues at the WTD 91 in the data acquisition, and for making available the data of the Eltro visibility meter. Participation by the Institute for Maritime Technology (IMT) in FESTER was funded by the South African Navy. Participation by TNO in FESTER was funded by the Royal Netherlands Navy through an OTWO contract.

6. REFERENCES

1. Holst, G. (1995). Electro-Optical Imaging System Performance. *Winter Park FL, JCD Publishing*, p337.
2. Berk, A., P. Conforti, R. Kennett, T. Perkins, F. Hawes & J. van den Bosch (2014). MODTRAN@6: A major upgrade of the MODTRAN@ radiative transfer code. *SPIE Proc.* **9088**, 9088H.
3. Hess, M., P. Koepke & I. Schult (1998). Optical properties of aerosols and clouds: the software package OPAC. *Bull. Am. Met. Soc.* **79**, 831-844.
4. Van Eijk, A.M.J., J.T. Kusmierczyk & J.P. Piazzola (2011). The Advanced Navy Aerosol

Model (ANAM): validation of small-particle modes. *SPIE Proc.* **8161**, 816108.

5. Piazzola, J.P & G. Tedeschi (2015). A model for the transport of sea-spray aerosols in the coastal zone. *Boundary-layer Meteorol.* **155**, 329-350.
6. Schaap, M., R.M.A. Timmermans, M. Roemer, G.A.C. Boersen, P.H.J. Bultjes, F.J. Sauter, G.J.M. Velders & J.P. Beck (2008). The Lotos-Euros model: description, validation and latest developments. *Int. J. Environment and Pollution* **32**, 270-290.
7. Van Eijk, A.M.J., J. Piazzola, G. Tedeschi & K. Stein (2016). Aerosol impacts on scene contrast. In Proc: International IR target and background modeling & simulation workshop (ITBMS).
8. Vogelbacher, S., A.M.J Van Eijk, D. Sprung, L. Cohen, E. Sucher & K. Stein (2016). Comparison of MODTRAN simulations and transmission measurements by path-integrated and in-situ techniques over a rural site in Northwestern Germany. *SPIE Proc.* **10002**, 1000203.
9. Van Binsbergen, S.A., P. Grossmann, F. February, L.H. Cohen. A.M.J. van Eijk & K. Stein (2017). In-situ and path-averaged measurements of aerosol optical properties. *SPIE Proc.* **10408**, 104080V.
10. Van Eijk, A.M.J, W.H. Gunter, F.J. February, B. Maritz, G. Vrahimis, M.S. Koago, C. Wainman, C. Eisele, D. Seiffer, E. Sucher, K. Stein, M. van Iersel, L.H. Cohen, S.A. van Binsbergen, H.J.M. Heemskerck, A. Sternberg, H. Schulte, A.D. van Rheenen, E. Brenthagen, J.B. Thomassen & D. Griffith (2016). The FESTER field trial. *SPIE Proc.* **9979**, 99790Q.
11. Sprung, D., Grossmann, P., Sucher, E., Weiss-Wrana K., & Stein, K. (2011). Stability and height dependent variations of the structure function parameters in the lower atmospheric boundary layer investigated from measurements of the long-term experiment VERTURM (vertical turbulence measurements). *SPIE Proc.* **8178**, 817809.
12. De Jong, A.N., Van Eijk, A.M.J., Cohen, L.H., Fritz, P.J., Gunter, W.H., Vrahimis G. & October, F.J. (2011). Application of year-round atmospheric transmission data, collected with the MSRT multiband transmissometer during the FATMOSE trial in the False Bay area. *SPIE Proc.* **8161**, 81610A.
13. De Jong, A.N., Schwering, P.B.W., Van Eijk, A.M.J. & Gunter, W.H. (2013). Validation of atmospheric propagation models in littoral waters. *Opt. Eng.* **52**, 046002.

14. Ullwer, C., D. Sprung, A.M.J. van Eijk, W.H. Gunter & K. Stein (2017). Inhomogeneity of optical turbulence over False Bay (South Africa). *SPIE Proc.* **10425**, 1042509.
15. Sprung, D, A.M.J. Van Eijk, W.H. Gunter, D. Griffith, C. Eisele, E. Sucher, D. Seiffer & K. Stein (2017). Investigation of the height dependency of optical turbulence in the surface layer over False Bay (South Africa). *SPIE Proc.* **10408**, 104080U.